A Smooth Uniting Controller for Robotic Manipulators: An Extension of the Adaptive Variance Algorithm (AVA)

Gianluca Garofalo and George Mesesan

***Abstract*— The compliant behavior that a robotic manipulator realizes in the proximity of the desired goal is typically undesirable when the robot starts far away from the goal itself. In the latter case, high gains can produce motor torques which are unfeasible or too dangerous for interactions with humans and the environment. In this paper, a control algorithm is proposed that guarantees smooth high-gain/low-gain transitions to accommodate both the local and global requirements. The building block for this method is the recently proposed Adaptive Variance Algorithm (AVA). The theoretical proof of the result is validated with experiments on a humanoid robot.**

I. Introduction

Many of the control schemes used in the robotic community are related to the classic proportional-differential (PD) control law. This is not unexpected since the state of the robot can be defined as given by the joint positions and velocities. Therefore, such control schemes use a proportional feedback of the robot state. Examples are the seminal work in [1] and many of the schemes in [2]. Typically, the gains of the PD action are designed by the robotic control engineers in order to guarantee the desired performance in a neighborhood of the desired goal, which can be a desired configuration or trajectory. Nevertheless, for configurations that are far away from the goal, this could often lead to a control variable that saturates the actuators. This represents one of the many trade-offs the designer is faced with, i.e., balancing the local and global performance of the control action.

A possible solution to this problem is to switch between two controllers. One for the local behavior in the proximity of the desired goal and the other for the global behavior [3]. These kind of schemes require a more advanced stability analysis and might lead to discontinuous control inputs. A related and commonly used procedure is also to interpolate a smooth trajectory between the start and final points, that the controller is later required to track. This is typically realized using, for example, a low-pass filter similar to those in [4]. The drawback of this approach is that the low-pass filter will affect the behavior of the system both in the proximity of the desired goal and far away from it, even though it is not necessary (and actually undesirable) to modify the behavior of the system near the goal. In other words, only when large control errors are amplified by the controller gains, the behavior should be altered. Moreover, the interpolation requires additional tuning and might decrease the performance of the system when tracking trajectories with high-frequency components. Other approaches do not specifically design a second controller for the global performance, but rather saturate the control input [5]–[8]. All of these references analyze the presence of saturation in the control scheme, since undesirable effects in the closed-loop system could arise if the saturation would simply be neglected.

The authors are with the Institute of Robotics and Mechatronics, German Aerospace Center (DLR), Wessling, Germany. gianluca.garofalo(at)dlr.de

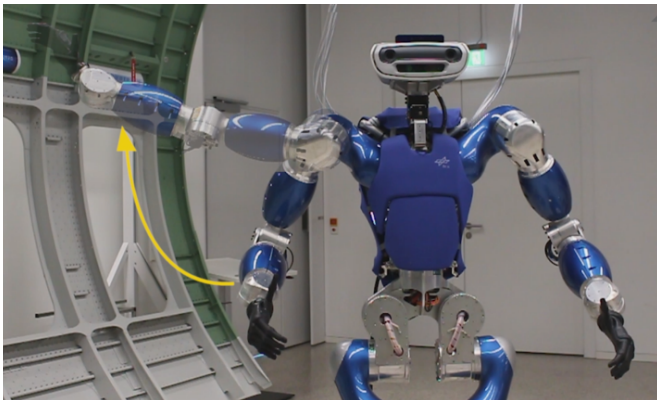

Fig. 1. Initial and final desired configuration of the humanoid robot TORO in the first experiment reported in the paper and video attachment [9].

In this paper, a dynamic state feedback for robotic manipulators is designed, which smoothly combines a local and global controller. The smooth transitions between the two controllers are realized via state-dependent gain transitions, following the design steps introduced in [10]. The key concept in [10] is that the nominal constant gain is multiplied by an adjustable windowing function, which adapts the value of the gain in an expanding or contracting neighborhood of the desired goal. As the windowing effect is realized by means of an unnormalized Gaussian function with an adaptive variance, the control algorithm in [10] was referred to as *Adaptive Variance Algorithm* (AVA). Compared to the cited saturated PD schemes, the proposed control law does not aim at guaranteeing that the hardware limitations are not exceeded, but rather to automatically adjust the gains depending on the error. This will reduce, as a byproduct, the likelihood of saturation. To guarantee that the input stays within its bounds, a saturation should be added as in the other methods. On the other hand, unlike the schemes which have predefined regions where the saturation acts, the adaptive nature of AVA allows the controller to automatically change its behavior. To visualize this phenomenon, imagine having a saturated spring torque. Far from the equilibrium, the local stiffness for the saturated scheme would be always (nearly) zero, while otherwise it has its nominal value. Therefore,

only these two stiffness values are possible. With AVA, instead, the stiffness is continuously adapted and is allowed to increase if a disturbance prevents the controller from reducing the error, given that the control input is within its bounds. This kind of scenario is considered in one of the reported experiments conducted with the robot in Fig. 1 and it can also be examined in the video attachment [9].

The main contribution of the paper can be summarized as a twofold extension of AVA. Firstly, the design is specialized for a robotic system in order to avoid feedback linearization and related model compensations by taking advantage of the mathematical structure of the mechanical model. Secondly, the combination of AVA with a global controller is presented. This is possible by noticing that the AVA formulation in [10] allows for a convex combination of controllers.

The paper is organized as follows. Section II presents the main idea of [10]. In Section III, the model and the control objective are presented. Section IV contains the main result, which is formalized as a theorem. The behavior of the control law during experiments with a humanoid robot is shown in Section V. Finally, Section VI summarizes the work.

A. Preliminaries

The usual Euclidean norm will be denoted by $|\cdot|$.

Global asymptotic stability will be denoted in short as GAS. By 0-GAS it is meant that the system $\dot{x} = f(x, 0)$ is GAS. This is the unforced system associated to the system with inputs $\dot{x} = f(x, u)$. Similarly, the letters U and B will be used to replace the words uniform and bounded, respectively. For example, UGB stands for uniformly globally bounded. Finally, ISS denotes input-to-state stability. When not specifically stated, these properties are always meant to hold for the origin of the state space.

II. The Adaptive Variance Algorithm

In this section, the application of the Adaptive Variance Algorithm (AVA) to a simple integrator is reviewed, in order to exemplify the idea behind the algorithm.

In the remainder, without loss of generality, the regulation to the origin of the state space will be considered.

Consider the single input integrator with state $\xi \in \mathbb{R}$

$$\dot{\xi} = v \ , \tag{1}$$

where $v \in \mathbb{R}$ is the control input to be chosen such that $\xi \to 0$ as $t \to \infty$. Clearly, $v = -k_1 \xi$, with $k_1 > 0$ achieves this control objective and renders the system GAS. The following theorem states that the same can be guaranteed also with a dynamic state feedback, which modifies the gain by an adaptive windowing function.

Theorem 1 ([10]): For the integrator system (1)*, the dynamic state feedback with internal state* $\sigma \in \mathbb{R}$

$$v = -k_1 e^{-V(\xi,\sigma)} \xi \tag{2a}$$

$$\dot{\sigma} = \left(k_3 - k_2 e^{-V(\xi,\sigma)}\right)\sigma \ , \tag{2b}$$

where, given the constant $\bar{\sigma} > 0$*,* $V : \mathbb{R}^2 \to \mathbb{R}$ *is defined as*

$$V(\xi, \sigma) = \frac{\xi^2}{2(\bar{\sigma}^2 + \sigma^2)} \tag{3}$$

leads to a GAS closed-loop system, provided that the gains satisfy the inequalities $k_1 > 0$ *and* $k_2 > k_3 > 0$*.*

Proof: See [10, Theorem 1]. ■

Given the expression of $V(\xi, \sigma)$, the term $e^{-V(\xi,\sigma)}$ is an unnormalized unimodal Gaussian function with zero mean and variance $\bar{\sigma}^2 + \sigma^2$. The idea behind (2) is to use a smooth windowing function to reduce the control effort far from the equilibrium point, i.e., for large control errors. Additionally, the internal state of the controller evolves to automatically adapt the windowing size and still yield a GAS system. The condition $k_2 > k_3 > 0$ intuitively guarantees that the windowing size starts shrinking back to its original value as the system approaches the goal. Although σ will eventually converge to zero, the dynamic in (2b) implies an exponential growth of σ for values that are far from $\xi = 0$. Here the word "far" denotes values outside the region defined by the variance of the Gaussian. Given an initial condition ξ_0 far from the origin, then $k_1 e^{-V(\xi,\sigma)}$ will be initially small and, as σ increases, it will tend to the nominal value k_1. On the other hand, the controller will approach the behavior of a static state feedback within a neighborhood of the origin. The size of such neighborhood is adjustable via $\bar{\sigma}$.

III. Robot model and control objective

The considered robotic systems are modeled by the nonlinear differential equations:

$$M(\xi)\ddot{\xi} + C(\xi, \dot{\xi})\dot{\xi} + g(\xi) = u \ , \tag{4}$$

where the state of the robot is given by generalized positions and velocities ξ, $\dot{\xi} \in \mathbb{R}^n$, n being the number of degrees of freedom (DoF). The variable ξ could represent, for example, robot joint angles or Cartesian positions[1]. The dynamic matrices are the symmetric and positive definite inertia matrix $M \in \mathbb{R}^{n \times n}$, a Coriolis matrix $C \in \mathbb{R}^{n \times n}$ satisfying the passivity property $\dot{M} = C + C^\top$ and the gravity torque vector $g \in \mathbb{R}^n$. Finally, the control input $u \in \mathbb{R}^n$ is realized through the motors of the robot.

The controller has to satisfy two requirements. The main control goal is the stabilization of a smooth desired trajectory $\xi_d(t)$, with available time derivatives. Therefore, $\tilde{\xi} \to 0$ as $t \to \infty$, with $\tilde{\xi} = \xi - \xi_d$. The second control requirement is to fulfill the stabilization objective while smoothly pass from a high-gain control action in a neighborhood of the desired trajectory (referred to as local controller) to a second control action (referred to as global controller) for large control errors and vice versa. Typically, the global controller is a low-gain or a saturated control action, in order to avoid large values of the control input.

IV. Main result

Before presenting a possible solution to the problem stated in Section III in the form of a theorem, it is useful to introduce the following notation. The i-th element of a vector or the i-th element on the diagonal of a matrix is given by ${}^i(\cdot)$. The identity matrix is denoted by I.

[1]Assuming a diffeomorphism between joint and Cartesian positions.

A. Local and global controllers

A proportional action will be used as local controller, of the type $v_l = -K_1\tilde{\xi}$, with $K_1 \in \mathbb{R}^{n\times n}$ diagonal and positive definite. In Section II, an unnormalized Gaussian function with adaptive variance was used as windowing function for this proportional action, so that a smooth transition to a low gain was realized far from the desired trajectory. Here, the same idea is used to allow for smooth transitions between the local and global controller. The purpose of the global controller is to avoid unfeasible or dangerous values of the control variable that can arise when the local controller is used far from the desired trajectory. For this reason, examples of global controllers that can be used are a smooth saturation ${}^i v_g(\tilde{\xi}) = -\,{}^i\tau_{max}\,\tau\tanh({}^i\tau_{max}^{-1}\,{}^iK_g\,{}^i\tilde{\xi}), \quad i \in \{1,\dots,n\}$, or another proportional action $v_g(\tilde{\xi}) = -K_g\,\tilde{\xi}$. Here, $\tau_{max} \in \mathbb{R}^n$ is the vector of the maximum torques and $K_g \in \mathbb{R}^{n\times n}$ a diagonal matrix, with $0 < {}^iK_g \ll {}^iK_1$.

B. Uniting controller

As in Section II, the controller itself is a dynamical system with internal state given by the vectors $\sigma,\ \rho \in \mathbb{R}^n$. The parameters of the controller are the vectors $\bar{\sigma},\ \bar{\rho} \in \mathbb{R}^n$ and the diagonal matrices $K_j,\ H_j \in \mathbb{R}^{n\times n}$ with $j \in \{1,2,3\}$. The design of the controller aims at bringing the closed-loop system in cascaded form. In the upstream subsystem, $\bar{\rho}$ and H_j will appear, while $\bar{\sigma}$ and K_j are in the downstream subsystem. In each subsystem the local proportional action will be combined with the global controllers $v_{g_2}(s)$ and $v_{g_1}(\tilde{\xi})$, respectively, where the variable s will be introduced shortly. These global controllers have the expression given in Section IV-A. The combination of the local and global controllers is realized via a convex combination. The coefficients of the combinations are $E_{\bar{\rho}}(s,\rho)$ and $I - E_{\bar{\rho}}(s,\rho)$ for the upstream subsystem and $E_{\bar{\sigma}}(\tilde{\xi},\sigma),\ I - E_{\bar{\sigma}}(\tilde{\xi},\sigma)$ for the downstream one. Both $E_{\bar{\sigma}}(\tilde{\xi},\sigma)$ and $E_{\bar{\rho}}(s,\rho)$ are diagonal matrices, with $E_{\bar{\sigma}}(\tilde{\xi},\sigma),\ E_{\bar{\rho}}(s,\rho) \in \mathbb{R}^{n\times n}$. Using the shorthand

$$ {}^iV_{\bar{\sigma}} = \frac{{}^i\tilde{\xi}^2}{2({}^i\bar{\sigma}^2 + {}^i\sigma^2)} \qquad {}^iV_{\bar{\rho}} = \frac{{}^is^2}{2\,({}^i\bar{\rho} + {}^i\rho^2)}\ , \tag{5} $$

the entries of $E_{\bar{\sigma}}(\tilde{\xi},\sigma)$ and $E_{\bar{\rho}}(s,\rho)$ are $e^{-{}^iV_{\bar{\sigma}}}$ and $e^{-{}^iV_{\bar{\rho}}}$, respectively. At this point, as in [11], the sliding variable $s \in \mathbb{R}^n$ and the reference velocity $\dot{\xi}_r \in \mathbb{R}^n$ are introduced

$$ s = \dot{\tilde{\xi}} + E_{\bar{\sigma}}(\tilde{\xi},\sigma)K_1\tilde{\xi} - \big(I - E_{\bar{\sigma}}(\tilde{\xi},\sigma)\big)v_{g_1}(\tilde{\xi}) \tag{6} $$

$$ \dot{\xi}_r = \dot{\xi} - s\ . \tag{7} $$

Therefore, $\ddot{\xi}_r = \ddot{\xi} - \dot{s}$ and it is a function of $\ddot{\xi}_d$, $\tilde{\xi}$, $\dot{\tilde{\xi}}$ and σ.

Theorem 2: Given the system (4)*, the variables* (6)*,* (7) *and the global controllers $v_{g_1}(\tilde{\xi})$, $v_{g_2}(s)$ satisfying ${}^i\tilde{\xi}\ {}^iv_{g_1}\,({}^i\tilde{\xi}) \le 0$ and ${}^is\ {}^iv_{g_2}\,({}^is) \le 0$, respectively, let*

$$ u = M(\xi)\ddot{\xi}_r + C(\xi,\dot{\xi})\dot{\xi}_r + g(\xi) + v \tag{8} $$

$$ v = -E_{\bar{\rho}}(s,\rho)H_1 s + \big(I - E_{\bar{\rho}}(s,\rho)\big)v_{g_2}(s)\ . \tag{9} $$

Then the closed-loop system (considering also the dynamics of the controller)

$$ M\dot{s} = -\big(C + E_{\bar{\rho}}H_1\big)s + \big(I - E_{\bar{\rho}}\big)v_{g_2} \tag{10a} $$

$$ \dot{\rho} = \big(H_3 - E_{\bar{\rho}}H_2\big)\rho \tag{10b} $$

$$ \dot{\tilde{\xi}} = -E_{\bar{\sigma}}K_1\tilde{\xi} + \big(I - E_{\bar{\sigma}}\big)v_{g_1} + s \tag{10c} $$

$$ \dot{\sigma} = \big(K_3 - E_{\bar{\sigma}}K_2\big)\sigma \tag{10d} $$

is UGAS provided that $K_j,\ H_j,\ j \in \{1,2,3\}$, are chosen such that they satisfy the inequalities ${}^iK_j > 0$, ${}^iH_j > 0$ and ${}^iK_2 > {}^iK_3 > 0$, ${}^iH_2 > {}^iH_3 > 0$, $i \in \{1,\dots,n\}$. Moreover, $\bar{\sigma}$ and $\bar{\rho}$ are used to influence the region for the transitions between the local and global controllers.

Proof: See Appendix II. ∎

Remark 1: Although the dependencies in (10) have been omitted for simplicity, note that (10) is non-autonomous, since the dynamic matrices depend on ξ and $\dot{\xi}$.

Remark 2: Due to the use of the sliding variable, as $s \to 0$, the system tends to behave like n systems of the type in Section II. The only difference compared to Section II is the presence of the global controller $v_{g_1}(\tilde{\xi})$. This means that, for large errors $\tilde{\xi}$, the behavior is given by $v_{g_1}(\tilde{\xi})$ rather than simply having a proportional action with reduced gain. The dynamics in (10a), instead, are fully coupled due to the presence of the dynamic matrices.

V. Validation

The experiments were conducted using the humanoid robot TORO [12]. Videos of the experiments presented in this section can be found in the multimedia attachment [9].

Two experiments are presented. For both, the global controllers v_{g_1} and v_{g_2} have been chosen to be a smooth saturation as described in Section IV-A. The proposed controller is used in combination with a whole-body control framework [13]. In particular, AVA is used to control only the six joints of the right arm, while the whole-body controller aims at providing an almost fixed base for the arm. The arm joints are denoted by q and are ordered from 1 to 6. The first three joints correspond to the shoulder, the fourth to the elbow and the last two to forearm and wrist, respectively.

In the first experiment, a step of the desired joint position q_d is commanded to four of the six joints of the arm. The values can be observed in Fig. 2 and the correspondent substantial change in the configuration of the robot is visible in Fig. 1. It is important to mention that without the local/global controller transitions realized via the adaptation of σ and ρ (see Fig. 3) such a considerable difference in q_d could not have been executed by the local controller alone. The torque limits would have been violated and the execution stopped.

The transitions between the local and global controllers are clearly visible when Fig. 2 is compared with Fig. 4. The latter shows the evolution of the windowing terms $E_{\bar{\sigma}}(\tilde{\xi},\sigma)$ and $E_{\bar{\rho}}(s,\rho)$. Two effects are noticeable. First, the transitions timing is different for each joint, because of the different commanded deflections and the different values of ${}^i\bar{\sigma}$. Second, due to the minimal change of ρ in Fig. 2, the values of $E_{\bar{\rho}}(s,\rho)$ in Fig. 4 are almost constantly one. The

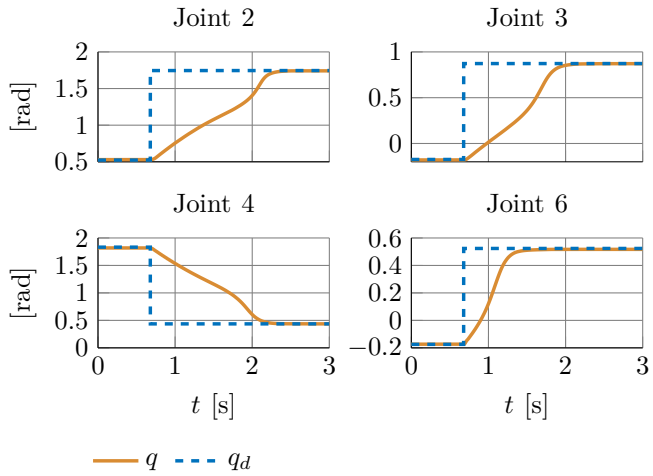

Fig. 2. Evolution of the measured and desired joint positions q and q_d during the first experiment with TORO. The corresponding desired robot configurations are visible in Fig. 1.

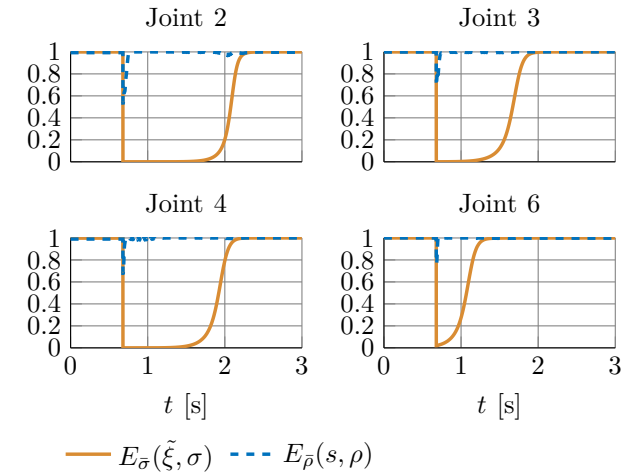

Fig. 4. Evolution of $E_{\bar{\sigma}}(\tilde{\xi}, \sigma)$ and $E_{\bar{\rho}}(s, \rho)$ during the first experiment with TORO. The global controller v_{g_2} is practically never active, as confirmed by the fact that ρ stays close to zero in Fig. 3.

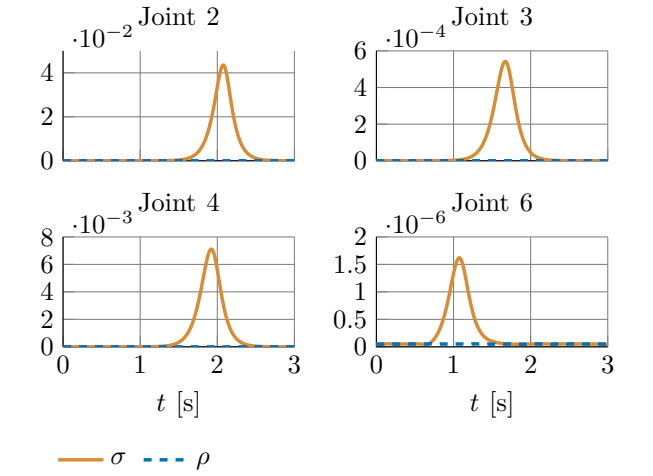

Fig. 3. Evolution of controller states σ and ρ during the first experiment with TORO. The change of σ causes the transitions between the local controller $K_1 \tilde{\xi}$ and the global controller v_{g_1}, see also Fig. 4.

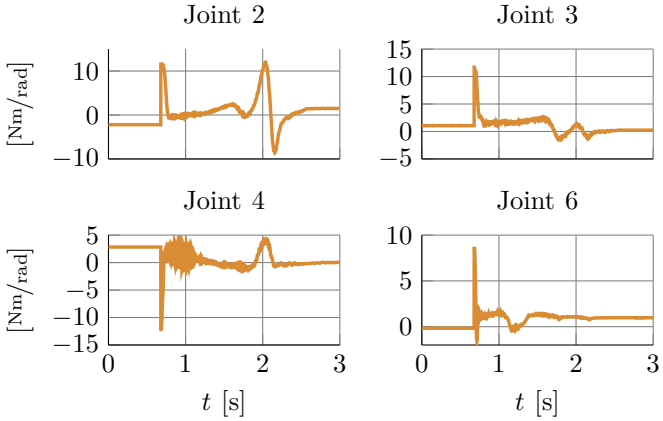

Fig. 5. Evolution of the torque input u during the first experiment with TORO. The values approach zero because the effects of gravity are already compensated by the whole-body controller, in which AVA is included.

reason is that a transition between local and global controller is not required given the value of $\bar{\rho}$. In the second experiment, these values are lowered to show the difference.

Finally, the evolution of the commanded torques is reported for completeness in Fig. 5. Notice that the values tend towards zero because the effects of gravity are already compensated by the whole-body framework used on TORO, in which AVA is included. Additional sources of noise are calibration errors, the fact that the hands of the robot are not included in the dynamic model and the effects of the whole-body controller. Although the latter is able to balance the robot, the base of the arm is not perfectly fixed.

In the second experiment, the comparison with a method using saturation is considered. For kinesthetic teaching, a PD control law with saturation was implemented on TORO [14]. In particular, the torque due to the stiffness term is saturated to avoid dangerous torque values during demonstration of the task by the human. While the simple saturation of the torque might be desirable in the teaching scenario, the goal of this experiment is to show that having predefined static regions for the transition to a saturated torque leads to a loss of GAS. Therefore, AVA is a better alternative when it is required to reach the desired goal. In the first phase of the experiment, a PD controller as in [14] is used and a weight is placed in the hand of the robot, which causes a deflection of the arm. Due to the saturation of the stiffness torque, the robot is unable to return to the initial position. At this point, the controller was switched to AVA. For this particular example, $\bar{\sigma}$ and $\bar{\rho}$ have been considerably lowered (by factor ten) to highlight the transition from the global to the local controller. Fig. 6 shows how the increase of σ and ρ corresponds to a transition from the global to local controller, which enable the reduction of the initial deflection caused by the previously active controller. Nevertheless, a residual deflection is still visible due to the unmodeled additional weight in the hand. Accordingly, σ and ρ do not go back

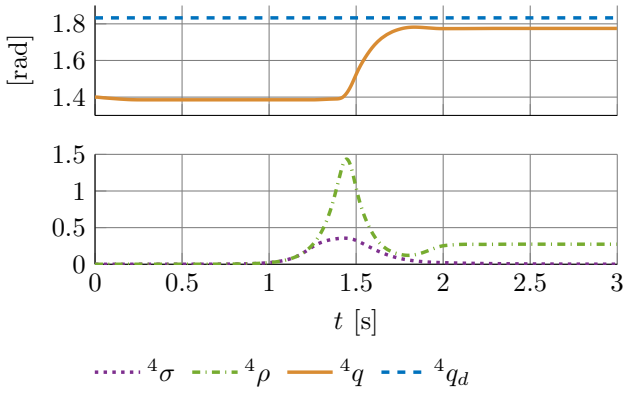

Fig. 6. Time evolution for the elbow of joint position and controller states during the second experiment. The controller is able to reduce the deflection initially caused by the previously active saturated PD by realizing the transition from global to local controller.

to zero since the windowing Gaussian has to remain open enough to allow for the local controller to compensate for the disturbance.

A final remark is on the role of the controller gains K_j, H_j with $j \in \{2, 3\}$. Their role was thoroughly investigated in [10] where AVA was first introduced. In short, they influence how rapidly the unnormalized Gaussian functions expand and contract. As a consequence, they influence the rate at which the local/global controller transitions are realized. In the experiments, these gains were chosen to have fast transitions in order to highlight the change from the global to local controller not only in the plots, but also in the video showing the execution of the robot motion [9].

VI. Conclusion

In this paper, a control law that guarantees global stabilizing capabilities for a robotic manipulator has been presented. In addition, the characteristic feature of the controller is the ability to realize a smooth transition between a local and a global controller relying on the recently proposed *Adaptive Variance Algorithm* (AVA). Therefore, the latter has been extended in two ways. Firstly, the passivity property of the robot is used instead of feedback linearization. Secondly, the behavior of the system far from the desired trajectory is no longer limited to a proportional state feedback with vanishing gains, but combined with a global controller. The stability of the algorithm is analyzed and experiments with a humanoid robot are used to validate and compare the theoretical results.

Appendix I

Useful theorems for the derivation of the results presented in this paper are reported here for completeness. The mappings are assumed to be locally Lipschitz in the state, uniformly in the time and to be zero at the origin of the state space. See also [15], [16].

Theorem 3 ([16]): The cascade system

$$\dot{x}_1 = f_1(t, x_1) \tag{11a}$$
$$\dot{x}_2 = f_2(t, x_2) + g(t, x_1, x_2)x_1 \ , \tag{11b}$$

is UGAS if and only if (11a) *is UGAS,* (11b) *is* 0*-UGAS and the solutions of* (11) *are UGB.*

Theorem 4 ([15]): If the positive real-valued, differentiable function $W(x)$, defined on B, is unbounded on any unbounded set and $\dot{W} \leq 0$ holds on the intersection of an end set with some set of the form $\{x \mid |x| \geq M > 0\}$, then all orbits starting in B are bounded in the future.

Appendix II

This appendix contains the proof of Theorem 2 and all the needed lemmas. To this end, define

$$z_1 = \begin{bmatrix} s^\top & \rho^\top \end{bmatrix}^\top \qquad z_2 = \begin{bmatrix} \tilde{\xi}^\top & \sigma^\top \end{bmatrix}^\top \ .$$

Then the closed-loop system (10) can be written as the following cascade interconnection

$$\dot{z}_1 = f_1(t, z_1) \tag{12a}$$
$$\dot{z}_2 = f_2(z_2) + Gz_1 \ , \tag{12b}$$

with G the selection matrix extracting s out of z_1. Note that the explicit dependency on the time t in (12a) comes from the dependencies of the dynamic matrices. The goal is to use Theorem 3 to show that (12), i.e., (10), is UGAS. The following lemmas are used to verify that the conditions of the theorem are fulfilled.

Since all the matrices in (10c)-(10d) are diagonal, let

$$^i\dot{z}_2 = {}^i f_2({}^i z_2) + {}^i G\, {}^i z_1 \tag{13}$$

be the i-th system in (12b), $i \in \{1, \ldots, n\}$.

Lemma 1: Given a bounded input z_1, for each of the systems (13) *in* (12b) *there exist $^iM > 0$, an end set $^i\mathcal{E}$ and a positive real-valued, differentiable and radially unbounded function $^i\mathcal{W}$, such that $^i\dot{\mathcal{W}} \leq 0$ holds on $^i\mathcal{E} \cap {}^i\Omega_M$, with $^i\Omega_M = \left\{{}^i z_2 \mid \left|{}^i z_2\right| \geq {}^i M\right\}$.*

Proof: Since the presence of the global controller $v_{g_1}(\tilde{\xi})$ does not affect the proof in [10, Theorem 1] due to the property $^i\tilde{\xi}\ {}^i v_{g_1}\,(^i\tilde{\xi}) \leq 0$, the proof of the lemma follows directly from [10]. ■

Lemma 2: The system (12b) *is* 0*-GAS provided that $^iK_1 > 0$ and $^iK_2 > {}^iK_3 > 0$, $i \in \{1, \ldots, n\}$.*

Proof: Since all the matrices in (10c)-(10d) are diagonal, then when $\boldsymbol{s} = \mathbf{0}$ the system is equivalent to n systems as in Section II, with the addition of the global controller $v_{g_1}(\tilde{\xi})$. Since the presence of $v_{g_1}(\tilde{\xi})$ does not affect the proof in [10, Theorem 1] due to the property $^i\tilde{\xi}\ {}^i v_{g_1}\,(^i\tilde{\xi}) \leq 0$, it can be concluded that (12b) is 0-GAS. ■

The next lemmas are devoted to prove that (12a) is UGAS. To this end, it is useful to rewrite (12a) itself as

$$\dot{s} = f_s(t, s) \tag{14a}$$
$$\dot{\rho} = f_\rho(s, \rho) \ , \tag{14b}$$

i.e., as a cascade interconnection. Following the same steps as in [18], it is easy to see that the cascade interconnection of a UGAS system and an ISS system is still UGAS [16]. Note that in (14a) the dependency on $\rho(t)$ has been included in the explicit dependency on time. Visually, this is sketched in Fig. 7, where the idea is similar to [17]. As before, since all

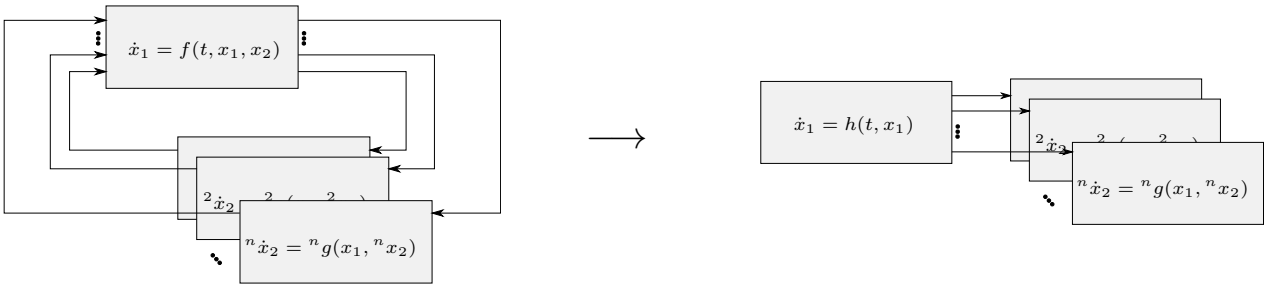

Fig. 7. Conceptual illustration of how a feedback interconnection with n systems can be seen as a cascaded interconnection. The idea is inspired by [17].

the matrices in (10b) are diagonal, each of the n systems in (14b) will be considered separately, i.e., with $i \in \{1, \dots, n\}$

$$ {}^i\dot{\rho} = \left({}^iH_3 - e^{-{}^iV_{\bar{\rho}}({}^is, {}^i\rho)} \ {}^iH_2 \right) {}^i\rho \ . \tag{15} $$

Lemma 3: Each system (15) *in* (14b) *is ISS with input* ${}^is$ *provided that* ${}^iH_2 > {}^iH_3 > 0$*,* $i \in \{1, \dots, n\}$*.*

Proof: See [10, Proof of Theorem 1]. ■

Lemma 4: The system (14a) *is UGAS, if* $H_1 > 0$*.*

Proof: Consider the function $U(t, s) = \frac{1}{2} s^\top M(t) s$. Let $\lambda_m > 0$ and $\lambda_M > 0$ be the smallest and largest[2] eigenvalue of $M(t)$, respectively. Then

$$ \frac{1}{2}\lambda_m |s|^2 \leq U(t, s) \leq \frac{1}{2}\lambda_M |s|^2 \tag{16} $$

$$ \begin{aligned} \dot{U}(t, s) &= s^\top \left[\left(I - E_{\bar{\rho}} \right) v_{g_2} - E_{\bar{\rho}} H_1 s \right] \\ &\leq -s^\top E_{\bar{\rho}} H_1 s \leq 0 \ , \end{aligned} \tag{17} $$

where the passivity property and ${}^is \ {}^iv_{g_2}({}^is) \leq 0$ have been used. Since the inequality (17) holds $\forall t \geq 0$, (14a) is UGB [19, Lemma A.8] and therefore it exists a $c > 0$ that is a lower bound for the exponentials in $E_{\bar{\rho}}$, such that $\forall t \geq 0$

$$ \dot{U}(t, s) \leq -c \, s^\top H_1 s \ . \tag{18} $$

Therefore (14a) is UGAS [20, Theorem 4.9]. ■

At this point, the proof of the main result can be given.

Proof: [Theorem 2] The system (12a) is UGAS because of Lemma 3-4. Additionally, (12b) is 0-GAS, see Lemma 2. The last step required by Theorem 3 is to show that (12) is UGB. This is possible, as in [10], thanks to Lemma 1 and the fact that (12a) is UGAS. Namely, using Theorem 4 in which the function ${}^iW$ is given by the sum of a Lyapunov function V for (12a) (which exists because the system is UGAS [16]) and ${}^i\mathcal{W}$ from Lemma 1, i.e., ${}^iW(z_1, {}^iz_2) = V(z_1) + {}^i\mathcal{W}({}^iz_2)$. Additionally, with $N > 0$, the end set is given by ${}^iE = \left\{ (z_1, z_2) \in \mathbb{R}^{4n} \mid |z_1| \leq N, \, z_2 \in \mathbb{R}^{2n} \right\} \cap {}^i\mathcal{E}$. By Theorem 4, each of the i-th cascade interconnection (12a)-(13) is UGB and therefore (12) is UGB. Finally, by Theorem 3, (12) is UGAS. ■

[2]The boundedness of the eigenvalue of $M(\xi)$ holds both in joint and Cartesian space. It is guaranteed by recognizing that the actual configuration space of a robot is bounded, due to the use of rotational joints or joints with end-stops. The property holds also in Cartesian space thanks to the assumption of a diffeomorphism between joint and Cartesian positions [19].

REFERENCES

[1] M. Takegaki and S. Arimoto, "A new feedback method for dynamic control of manipulators," *Journal of Dynamic Systems, Measurement, and Control*, vol. 103, no. 2, pp. 119–125, 1981.

[2] B. Siciliano, L. Sciavicco, L. Villani, and G. Oriolo, *Robotics: Modelling, Planning and Control*. Springer Publishing Company, Incorporated, 2008.

[3] R. G. Sanfelice and C. Prieur, "Robust supervisory control for uniting two output-feedback hybrid controllers with different objectives," *Automatica*, vol. 49, no. 7, pp. 1958–1969, 2013.

[4] J. A. Farrell, M. Polycarpou, M. Sharma, and W. Dong, "Command filtered backstepping," *IEEE Trans. on Automatic Control*, vol. 54, no. 6, pp. 1391–1395, 2009.

[5] I. V. Burkov and L. B. Freidovich, "Stabilization of the position of a lagrangian system with elastic elements and bounded control, with and without measurement of velocities," *Journal of Applied Mathematics and Mechanics*, vol. 61, no. 3, pp. 433–441, 1997.

[6] R. Kelly, V. Santibáñez, and H. Berghuis, "Point-to-point robot control under actuator constraints," *Control Engineering Practice*, vol. 5, no. 11, pp. 1555–1562, 1997.

[7] W. E. Dixon, M. S. D. Queiroz, F. Zhang, and D. M. Dawson, "Tracking control of robot manipulators with bounded torque inputs," *Robotica*, vol. 17, no. 2, pp. 121–129, 1999.

[8] A. Zavala-Rio and V. Santibanez, "A natural saturating extension of the pd-with-desired-gravity-compensation control law for robot manipulators with bounded inputs," *IEEE Trans. on Robotics*, vol. 23, no. 2, pp. 386–391, 2007.

[9] [Online]. Available: http://bit.ly/ACC2020_Garofalo_Mesesan

[10] G. Garofalo, "Global asymptotic stabilization with smooth high-gain/low-gain transitions: AVA - adaptive variance algorithm," *IFAC-PapersOnLine*, vol. 52, no. 16, pp. 25–30, 2019, 11th IFAC Symposium on Nonlinear Control Systems NOLCOS 2019.

[11] J.-J. E. Slotine and W. Li, "On the adaptive control of robot manipulators," *Int. Journal of Robotics Research*, vol. 6, pp. 49–59, 1987.

[12] J. Englsberger, A. Werner, C. Ott, B. Henze, M. A. Roa, G. Garofalo, *et al.*, "Overview of the torque-controlled humanoid robot TORO," in *IEEE/RAS Int. Conf. on Humanoid Robots*, Madrid, Spain, Nov. 2014, pp. 916–923.

[13] G. Mesesan, J. Englsberger, G. Garofalo, C. Ott, and A. Albu-Schäffer, "Dynamic walking on compliant and uneven terrain using DCM and passivity-based whole-body control," in *IEEE/RAS Int. Conf. on Humanoid Robots*, Toronto, Canada, Oct. 2019, pp. 25–32.

[14] D. Lee and C. Ott, "Incremental kinesthetic teaching of motion primitives using the motion refinement tube," *Autonomous Robots*, vol. 31, no. 2, pp. 115–131, 2011.

[15] P. Seibert and R. Suarez, "Global stabilization of nonlinear cascade systems," *Systems & Control Letters*, vol. 14, no. 4, pp. 347–352, 1990.

[16] A. Loría and E. Panteley, *Cascaded Nonlinear Time-Varying Systems: Analysis and Design*. London: Springer London, 2005, pp. 23–64.

[17] A. Loría, "From feedback to cascade-interconnected systems: Breaking the loop," in *IEEE Conf. on Decision and Control*, Cancun, Mexico, Dec. 2008, pp. 4109–4114.

[18] E. D. Sontag, "Further facts about input to state stabilization," *IEEE Trans. on Automatic Control*, vol. 35, no. 4, pp. 473–476, 1990.

[19] C. Ott, *Cartesian Impedance Control of Redundant and Flexible-Joint Robots*, ser. Springer Tracts in Advanced Robotics. Berlin: Springer-Verlag, 2008.

[20] H. K. Khalil, *Nonlinear Systems*. New Jersey: Prentice Hall, 2002.